Pakistan J. Zool., vol. 54(3), pp 1439-1442, 2022 DOI: https://dx.doi.org/10.17582/journal.pjz/20200730120707

Short Communication

Synthesis and Characterization of Porous β-Calcium Pyrophosphate Bone Scaffold Derived from Avian Eggshell

Ali Ghazi Atiyah[1]*, Nadia Hameed Rija Al-Falahi[2] and Ghazi Atiya Zarraq[3]

[1]*Department of Surgery and Obstetrics, Collegeof Veterinary Medicine, University of Tikrit, Tikrit, Iraq*

[2]*Department of Surgery and Obstetrics, College of Veterinary Medicine, University of Baghdad, Baghdad, Iraq.*

[3]*Department of Applied Geology, University of Tikrit, Tikrit, Iraq*

ABSTRACT

Beta calcium pyrophosphate (β-CPP) scaffold, a type of calcium phosphate-based biomaterials, can be used in orthopedic and dental surgery. This study focused on the synthesis of the β-CPP bone scaffold from waste biomaterials such as avian eggshell, which consider a natural source of calcium precursor. The β-CPP powder was prepared by a wet precipitation process using calcination temperature 1200 ºC for 2 h, then the scaffold was designed by using cylindrical template under specific compression pressure. Synthesis of β-CPP powder was characterized by X-ray diffraction, Fourier transform infrared spectroscopy, scanning electron microscopy, and simulation body fluid. The results reveal that β-CPP powder was pure, well crystallinity and the designed scaffold had multiparous surface with pillars particles morphology, with Ca/P ratio (0.8) which matched with theoretical predictions. Also, there was a formation of rough precipitation layer when using SBF showed the bioactivity of the scaffold. Finally, the β-CPP scaffold was successfully synthesized from avian eggshell waste with high purity and favourite biocompatibility which was promising for use as bone substitution materials.

Article Information
Received 30 July 2020
Revised 11 September 2020
Accepted 04 December 2020
Available online 20 May 2021 (early access)
Published 04 March 2022

Authors' Contribution
AGA and NHRA designed the study and conducted the research. GAZ analysed the data and wrote the manuscript.

Key words
Calcium pyrophosphate, Eggshell, Bone scaffold

Many orthopedic surgeons look for suitable bone graft biomaterials intended to eliminate the need for autograft, allografts, or xenografts, which carry critical morbidity, complication, high cost, extended surgical time and immune rejection (Yuan *et al*., 2010). Calcium phosphate-based biomaterials have been effectively used over 40 years as essential raw materials for replacing or promoting the healing of the hard tissue (Zhang *et al*., 2014). Recently calcium phosphate bioapatite with osteoconductive and bioresorbable properties due to its similarity with mineral phase of bone and biological safety for the living body without any toxicity have received attention (Kang *et al*., 2017). It is now used as bone substitution materials in orthopedic and dental surgery. These material also have the same properties to induce inflammatory cellular responses (Velard *et al*., 2013). In addition, the calcium phosphate bioapatite scaffold is economic and with a few complications at the implanted site (Hernigou *et al*., 2017).

Hydroxyapatite (HA) and tricalcium phosphate (TCP) are also well-known as bone substitution biomaterial because of their biocompatibility and osteoinductivity properties (Zhang *et al*., 2014). They have moderate degradation (Arcos *et al*., 2014). On the other hand, calcium pyrophosphate (CPP) possesses all the properties required for biomaterial scaffold such as the desirable osteoconductivity, biocompatible and nontoxic effects which can be used as an alternative material for bone repairing (Tadic and Epple, 2004).

The aim of this stusy is to demonstrate the synthesis and evaluation of pure CPP scaffold by using avian eggshell waste as the natural source of calcium precursor.

Materials and methods

The CPP powder was synthesis from waste eggshell by using modified Holanda (2016). Concisely, the uncrushed eggshells were washed with deionized water several times, followed by boiling in water for 30 min to remove shells membrane and any debris. Then dried in the oven at 100°C for 30 min. The eggshell calcium carbonate powder was dissolved in nitric acid (1 mol/L) with continuous stirring for 2 h. A drop of Na_2HPO_4 was gradually added to the $Ca(NO3)_2$ solution thoroughly on magnetic stirrer at 50 ºC for 2 h. The precipitate was rapidly filtered and twice washed with deionized water, then left dried at room temperature overnight. Finally, the dried powder was calcined in a muffled furnace at 1200 ºC for 2 h. The produced powder was crushed to a fine powder (10µm) with a laboratory mortar grinder (Retech-

* Corresponding author: alighazivet@tu.edu.iq
0030-9923/2022/0003-1439 $ 9.00/0

Rm200, India), and put into scaffold design templet cylinders with a diameter of 5 mm. and then applying 40 MPa. electromechanical pressure compression using (MTI-40MPA-USA) to manufacture of a bone scaffold (Atiyah *et al*., 2018).

X-Ray Diffraction (XRD) was used to detect the phases and purity of β–CPP. A small sample (150 mg) of powdered was deposited in a holder for XRD. The powder samples were placed in a diffractometer (Crystalloflex diffractometer, D- 500, Siemens. Germany) using intensity rang from (zero to 1000) and diffraction angle (2θ) range from (20 – 60 degree).

The functional groups of the β–CPP present in the prepared powder was recorded on Fourier-Transform Infrared (FTIR) spectrophotometer (Shimadzu-8400S-Japan) using infrared from ranging from (400 to 4000 cm-1).

To reveal the structure and morphology of the β-CPP scaffold by using SEM analyses (Tuscan Vega 3rd Generation-England). The image made at a magnification ×10 allowed us to observe the particles size and surface porosity. The energy depressive spectroscopy also achieved by using the same SEM to known the minerals contents of scaffold and determined the calcium to phosphor (Ca;P) ratio.

The bioactivity of the scaffold was evaluated by using simulation body fluid (SBF). The SBF was prepared closed to chemical combinations of human blood plasma, with different ions concentrations similar to the inorganic compositions of human blood pH. SBF was prepared using Kokubo procedure (Ã and Takadama, 2006) and to observe any appearance of calcium phosphate spherulites layers on the scaffold surface.

Results and discussion

The diffraction pattern of the prepared powder sample was similar to the standard (JCPDS card number/ 09-0346). The main diffraction peaks were observed at 29.57, 34.27 and 47.28 at 2θ angle corresponding to 008, 125 and 129 Miller indices, respectively. These sharp and narrow peaks indicated the complete crystallinity of β-CPP powder. However, smallest peaks indicated low crystanality related to blemish of some phase of minerals such as (CaCO3), lime (CaO) and other bioapatite. The average size of the crystallite powder measured by the Scherer's equation was found to be 444nm (Fig. 1).

The reflections of XRD matched closely with the standard reflections of β-CPP (JCPDS No. 09-0346). The appearance of patterns peaks in the XRD powder at 1200 ºC became sharp and narrow which indicated increase in the purity of the powder. This is similar to that of Zyman *et al*. (2017) who mentioned that increase in the calcinated temperature over 800 ºC lead to an increase in the purity of CPP by appearance of sharp peaks patterns and also the high calcinated temperature has a major role in the purity of powder product by conversion the powder from amorphous phase to well crystalline phase. The average crystallite size of the β-CPP powder calculated by the Scherer's formula was found to be 444 nm, and it is reported that crystallite size growth with increasing calcination temperature (Berent *et al*., 2019), thus the implant with large particle size have favorable results by leaving suitable porosity between these particles specially after compression process to produce the β-CPP implant. This leads to enhanced interactions with biological fluids and cells and accelerates peri-implant bone healing as well as improves osseointegration at the implantation sites in vivo (Zhang *et al*., 2014).

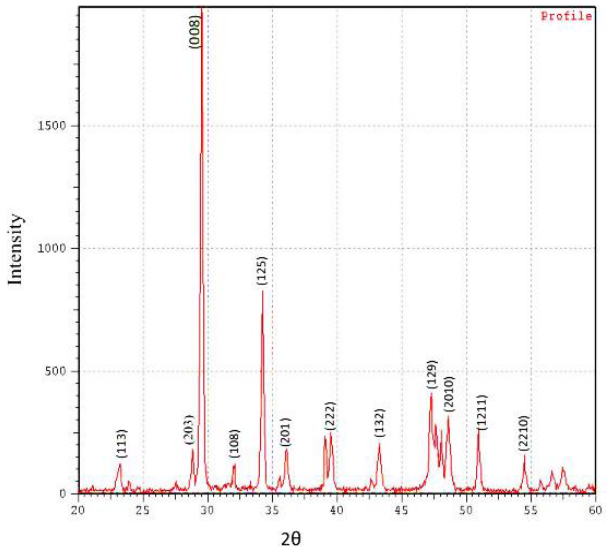

Fig. 1. XRD spectra of β-CPP powder calcinated at 1200°C for 2h at 2θ range from 20-60 degree and intensity range from zero- 1000.

The FTIR spectrum of β-CPP powder sample shows only the characteristics absorption bands of β-CPP. The prepared powder of β-CPP identified by the absorption spectrum of phosphate ions (PO_4^{3-}) groups at bands from 453.24cm^{-1} to 613.32cm^{-1}. The presence of stretching bands at 727.11cm^{-1} indicated the presence of HPO_4^{2-} group. Also the bands from 1000 to 1200 cm^{-1} were assigned to vibration of PO_4^{3-} and HPO_4^{2-} groups. The bands from 1400 to 1800 cm^{-1} referred to carbonate ions ($CO3^{2-}$) group. The region from 2400- 3200 cm^{-1} indicated the appearance of adsorbed water. The FTIR spectra also indicated the presence of peaks at 3600 cm^{-1} to 4000cm^{-1} which indicated to the presence of hydroxyl (OH^-) group (Fig. 2).

According to FTIR evaluation all of the functional groups were related to typical CPP stretching and bending phases which were similar to the results that presented

by Holanda (2016). In addition, a peak 1000 to 1200 cm^{-1} related to asymmetric extending of P-O-P bending modes, while, the band from 453.24cm^{-1} to 613.32cm^{-1} corresponds to symmetric P-O-P stretching of PO_4^{3-} ion this result agrees with the results mentioned by Vasant and Joshi (2011).

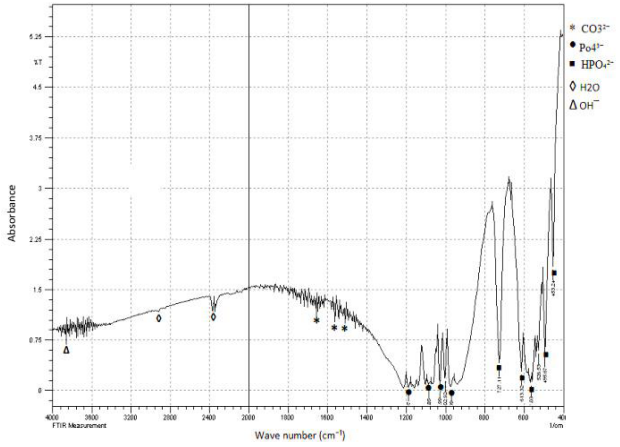

Fig. 2. FTIR spectra with wave length range from 400-4000 and absorbance rate rang from zero- 6.25 which shows the functional groups of β-CPP powder that calcinated at 1200°C for 2h.

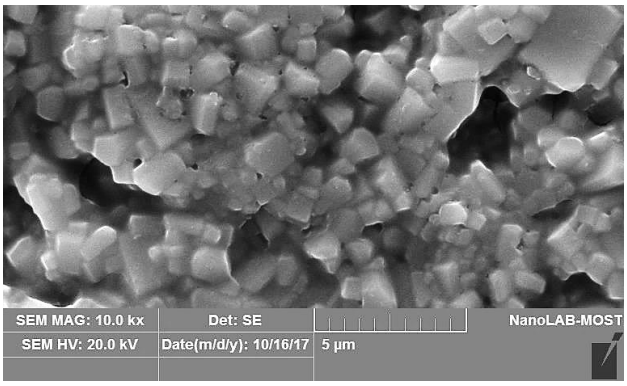

Fig. 3. SEM micrograph of β-CPP scaffold at magnification 10.0kx.

The SEM analysis showed micrographs of an eggshell β-CPP scaffold produced at a calcination temperature of 1200 °C. The SEM shows the morphology of particle which appear agglomerated pillars in shape with the particles variable in size range from 2 to 4 µm with the pore size approximately 4 µm. forming clusters of agglomerates that tend to leave a random and irregular multi-pores in between (Fig. 3). The purity and the Ca/P ratio of the β-CPP scaffold was also confirmed by SEM-EDS analysis that shows the existence of main mineral elements such as oxygen, phosphor and calcium of scaffold sample and the Ca/P ratio to be 0.8 (Fig. 4 and Table I).

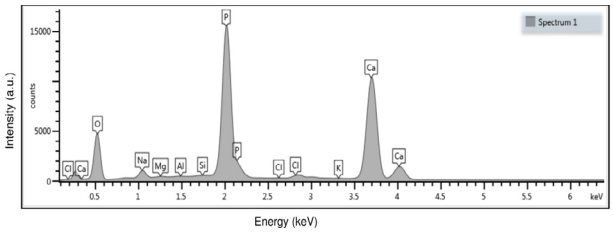

Fig. 4. EDX spectra shows the mineral elements of β-CPP scaffold.

Table I. EDS analysis of minerals elements contain in β-CPP scaffold sample.

Element	Weight %
O	41.67
Na	2.65
Mg	0.15
Al	0.24
Si	0.23
P	29.45
Cl	1.46
K	0.38
Ca	23.77
Total:	100.00

The uneven porosity within the scaffold sample causes the roughness on the surface by Safronova *et al*. (2017). Also the presence of surface porosity of the scaffold can enhance revascularization and bone remodeling, allowing the cells proliferation and improving biocompatibility when it is used as a bone implant *in vivo* (Hwang *et al*., 2013). Therefore, the porosity considers key point for bioactivity of calcium phosphate scaffolds. The Ca/P ratio (1.20) detected by EDX was close to the presumed value of β-CPP which is 1.000 (Holanda, 2016). The calcium phosphate-based materials were considered as biocompatible at a Ca:P proportion between 1:l and 2:0, because this ratio is favorable for bone cells activity *in vivo* (Liu *et al*., 2008). Salimi (2017) reported the Ca/P ratio of scaffold decreased as melting temperature elevated, which decrease from 1.06 to 0.88, and these ration are closer to Ca/P ratio of the present study (Salimi, 2017).

The immersion of the scaffold in the SBF solution indicate precipitate of an apatite layer on the surface of scaffold due to chemical reaction between cations and anions (Fig. 5A and B). After immersion of CPP sample within SBF at 36.5 1ºC for 14 days, the positive Ca^{2+} ions from SBF are attracted by the OH− and PO_4^{3-} ions present on β-CPP sample surface. The increased positive charge on the surface attracts more negatively charged hydroxyl (OH−) and phosphate (PO_4^{3-}) ions from the SBF solution, leading to precipitation of the apatite layer on the surface of sample (Chemistry, 1998). The size and thickness of

apatite layer increased with increasing SBF immersion time (Sooksaen *et al*., 2015). The formation of an appetite layer is important for integration of the implanted biomaterials scaffolds within the host bony tissues (Zadpoor, 2014). Although, we found that the SBF has the bone-bonding bioactivity suggesting formation of a bone-like irregular apatite layer on the surface of the scaffold.

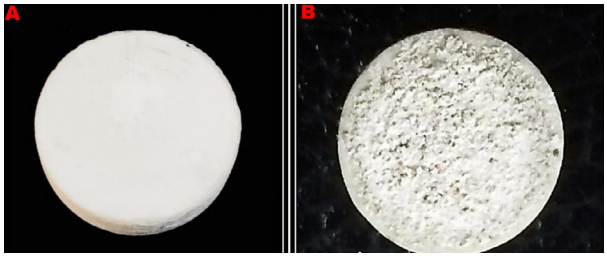

Fig. 5. The surface of the β-CPP sample. (A) before immersion in SBF, (B) after two weeks of immersion in SBF.

Conclusion

The β-CPP, considered an intermediate phase bioactive apatite ceramic between HA and β-TCP can be synthesis by simple and low cost method with waste eggshell as natural calcium precursor source. XRD illustrated the characteristic peaks phase of the synthesized β-CPP powder. FTIR showed the appearance of the characteristics bands of β-CPP. SEM also mentioned that the morphology of particles presented pillars in shape which depicts a typical partial morphology of β-CPP. On the other hand, the simulation body fluid reveals the biocompatibility of scaffold throughout the precipitation of rough, irregular layer on the surface of the scaffold that indicated good chemical reaction between SBF and surface of the scaffold. These outcomes very much the key component in the future attempt to overcome suitable β-CPP scaffold for all type of bones by using three dimensional printing designer machine for the structure of β-CPP bones and vertebrae templets.

Acknowledgements

The authors thank the Materials Research Service, Department of Science and Technology, Iraqi Ministry of Higher Education and Scientific Research, for supporting this research work.

Statement of conflict of interest

The authors have declared no conflict of interest.

References

Ã, T.K., and Takadama, H., 2006. *Biomaterials,* **27**: 2907–2915. https://doi.org/10.1016/j.biomaterials.2006.01.017

Arcos, D., Boccaccini, A.R., Bohner, M., Díez-pérez, A., Epple, M. and Gómez-barrena, E., 2014. *Acta Biomater.*, **10**: 1793–1805.

Atiyah, A., Al-Falahi, N. and Fadhil, K., 2018. *J. Vet. Res.*, **22**: 486491.

Berent, K., Komarek, S., Lach, R. and Pyda, W., 2019. *Materials*, **12**: 34766. https://doi.org/10.3390/ma12213476

Chemistry, M., 1998. *Acta Biomater.*, **46**: 2519-2527. https://doi.org/10.1016/S1359-6454(98)80036-0

Hernigou, P., Dubory, A., Pariat, J., Potage, D., Roubineau, F., Jammal, S. and Lachaniette, C.H.F., 2017. *Morphologie*, https://doi.org/10.1016/j.morpho.2017.03.005

Holanda, J.N.F., 2016. *Cerâmica*, **62**: 278–280. https://doi.org/10.1590/0366-69132016623631986

Hwang, N.S., Varghese, S., Lee, H.J., Zhang, Z. and Elisseeff, J., 2013. *Tissue Eng. Part A*., **19**: 15-16. https://doi.org/10.1089/ten.tea.2013.0064

Kang, K.R., Piao, Z.G., Kim, J.S., Cho, I.A., Yim, M.J., Kim, B.H., Oh, J.S., Son, J.S., Kim, C.S., Kim, D.K., Lee, S.Y. and Kim, S.G., 2017. *Implant Dentist.*, **26**: 378–387. https://doi.org/10.1097/ID.0000000000000559

Liu, H., Yazici, H., Ergun, C., Webster, T.J. and Bermek, H., 2008. *Acta Biomater.*, **4**: 1472–1479. https://doi.org/10.1016/j.actbio.2008.02.025

Safronova, T.V., Kurbatova, S.A., Shatalova, T.B., Knotko, A.V., Yevdokimov, P.V. and Putlyayev, V.I., 2017. *Inorg. Mater. appl. Res.*, **8**: 118–125. https://doi.org/10.1134/S2075113317010348

Salimi, E., 2017. *IOP Conf. Ser. Mater. Sci. Eng.,* **172**: Article number 012058.

Sooksaen, P., Pengsuwan, N., Karawatthanaworrakul, S. and Pianpraditkul, S., 2015. *Adv. Condens. Matter Phys.*, 2015. https://doi.org/10.1155/2015/158582

Tadic, D. and Epple, M., 2004. *Biomaterials*, **25**: 987–994. https://doi.org/10.1016/S0142-9612(03)00621-5

Vasant, S.R. and Joshi, M.J., 2011. *Mod. Phys. Lett. B.*, **25**: 53–62. https://doi.org/10.1142/S0217984911025419

Velard, F., Braux, J., Amedee, J. and Laquerriere, P., 2013. *Acta Biomater.*, **9**: 4956–4963. https://doi.org/10.1016/j.actbio.2012.09.035

Yuan, H., Fernandes, H., Habibovic, P., Boer, J. De, Barradas, A.M.C. and Ruiter, A.D., 2010. *Proc. natl. Acad. Sci. USA,* **107**: 10–15. https://doi.org/10.1073/pnas.1003600107

Zadpoor, A.A., 2014. *Mater. Sci. Eng. C.*, **35**: 134–143.

Zhang, J., Liu, W., Schnitzler, V., Tancret, F. and Bouler, J.M., 2014. *Acta Biomater.*, **10**: 1035–1049. https://doi.org/10.1016/j.actbio.2013.11.001

Zyman, Z., Goncharenko, A. and Rokhmistrov, D., 2017. *J. Cryst. Growth*, **478**: 117–122.